

Hierarchical assembly of Ag₄₀ nanowheel ranging from building blocks to diverse superstructure regulation

Received: 17 May 2024

Accepted: 9 October 2024

Published online: 23 October 2024

Xue-Jing Zhai¹, Meng-Yu Luo¹, Xi-Ming Luo¹ , Xi-Yan Dong^{1,2} , Yubing Si¹ ,
Chong Zhang¹, Zhen Han¹, Runping Han¹, Shuang-Quan Zang¹  &
Thomas C. W. Mak^{1,3} 

Authors and Affiliations

College of Chemistry, Zhengzhou University, Zhengzhou, 450001, China

Xue-Jing Zhai, Meng-Yu Luo, Xi-Ming Luo, Xi-Yan Dong, Yubing Si, Chong Zhang, Zhen Han, Runping Han, Shuang-Quan Zang & Thomas C. W. Mak

College of Chemistry and Chemical Engineering, Henan Polytechnic University, Jiaozuo, 454003, China

Xi-Yan Dong

Department of Chemistry, The Chinese University of Hong Kong, Shatin, New Territories, Hong Kong, SAR, China

Thomas C. W. Mak

Samapti Mondal

23.11.2024

Background

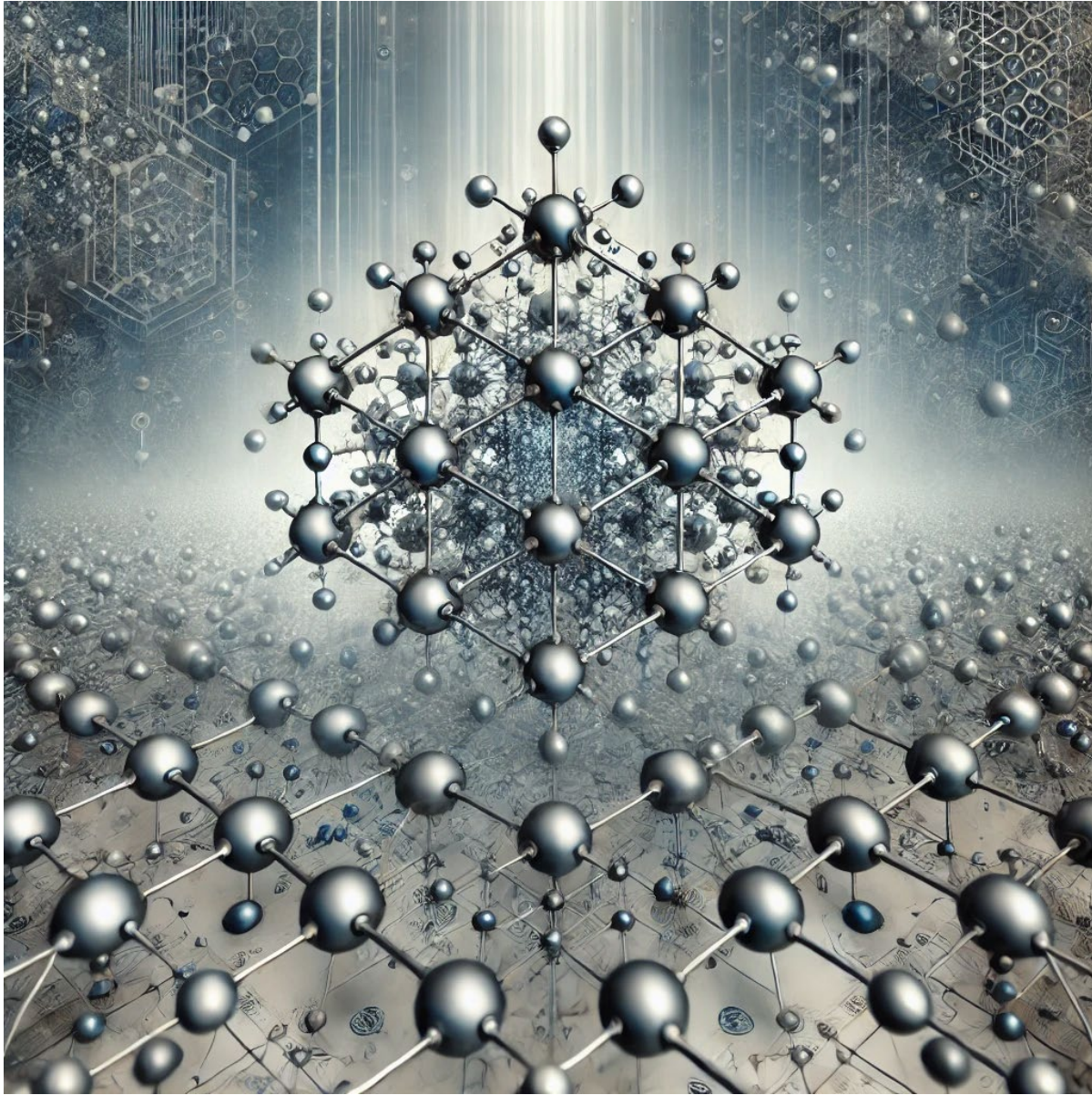
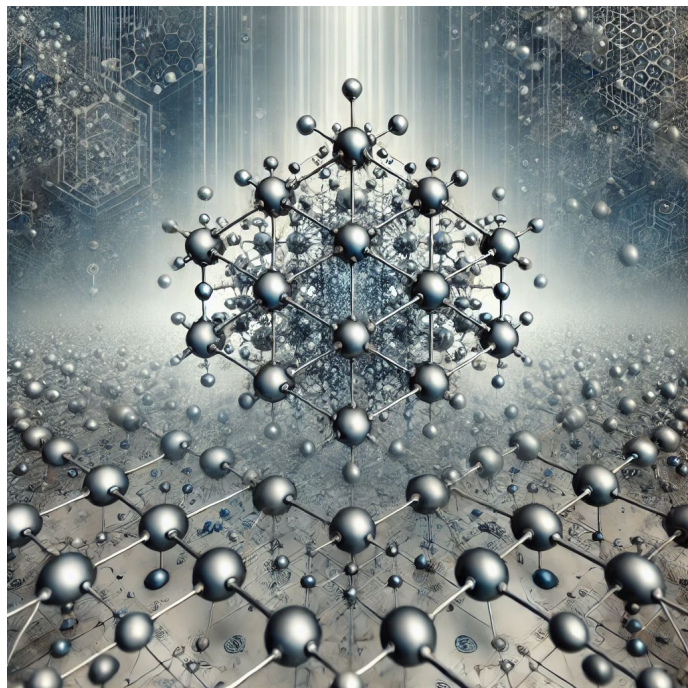


Image source: ChatGPT

Background



Chemical Reviews > Vol 118/Issue 24 > Article

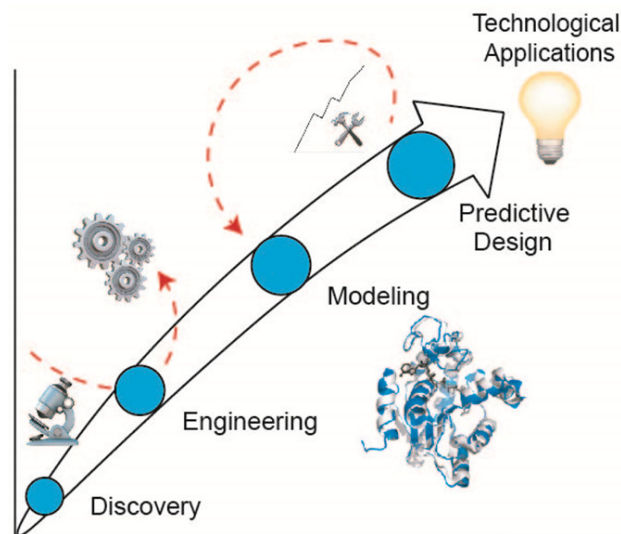
Subscribed

[Cite](#)
[Share](#)
[Jump to](#)
[Expand](#)

REVIEW | October 3, 2018

Biomolecular Assemblies: Moving from Observation to Predictive Design

Corey J. Wilson, Andreas S. Bommaris, Julie A. Champion, Yury O. Chernoff, David G. Lynn, Anant K. Paravastu, Chen Liang, Ming-Chien Hsieh, and Jennifer M. Heemstra*



Material Synthesis via Particle Assembly

Current: Manipulation of Nanoscale Structure

Next Generation Challenges



Enlargement	Fabrication
Integration	Transformation

Journal of the American Chemical Society > Vol 144/Issue 8 > Article

Subscribed

PERSPECTIVE | February 16, 2022

Nanoparticle Assembly as a Materials Development Tool

Margaret S. Lee, Daryl W. Yee, Matthew Ye, and Robert J. Macfarlane*

Double-helical assembly of heterodimeric nanoclusters into supercrystals

[Yingwei Li](#), [Meng Zhou](#), [Yongbo Song](#), [Tatsuya Higaki](#), [He Wang](#) & [Rongchao Jin](#) 

Nature **594**, 380–384 (2021) | [Cite this article](#)

Nanoscale
Horizons



COMMUNICATION

[View Article Online](#)

[View Journal](#) | [View Issue](#)



Cite this: *Nanoscale Horiz.*, 2021, 6, 913

Received 21st June 2021,
Accepted 19th August 2021

A double helical 4H assembly pattern with secondary hierarchical complexity in an Ag₇₀ nanocluster crystal[†]

Tao Chen,^a Sha Yang,^b Qinzhen Li,^a Yongbo Song,^c Guang Li, ^{*a} Jinsong Chai^{*c} and Manzhou Zhu ^{*bc}

Journal of the American Chemical Society > Vol 144/Issue 50 > Article

[Subscribed](#)



Cite Share Jump to

ARTICLE | December 9, 2022

Triple-Helical Self-Assembly of Atomically Precise Nanoclusters

[Hao Li](#), [Pu Wang](#), [Chen Zhu](#), [Wei Zhang](#), [Meng Zhou](#), [San Zhang](#), [Chunfeng Zhang](#), [Yapei Yun](#), [Xi Kang*](#), [Yong Pei*](#), and [Manzhou Zhu*](#)

Supercrystal engineering of atomically precise gold nanoparticles promoted by surface dynamics

[Qiaofeng Yao](#), [Lingmei Liu](#), [Sami Malola](#), [Meng Ge](#), [Hongyi Xu](#), [Zhennan Wu](#), [Tiankai Chen](#), [Yitao Cao](#),

[María Francisca Matus](#), [Antti Pihlajamäki](#), [Yu Han](#) , [Hannu Häkkinen](#)  & [Jianping Xie](#) 

Nature Chemistry **15**, 230–239 (2023) | [Cite this article](#)

Inorganic Chemistry > Vol 60/Issue 12 > Article

[Subscribed](#)

  
Cite Share Jump to

ARTICLE | June 3, 2021

[Cu{SC(O)OⁱPr}]₉₆: A Giant Self-Assembled Copper(I) Supramolecular Wheel Exhibiting Photoluminescence Tuning and Correlations with Dynamic Solvation and Solventless Synthesis

[Arvind K. Gupta](#), [Pilli V. V. N. Kishore](#), [Jhih-Yu Cyue](#), [Jian-Hong Liao](#), [Welni Duminy](#), [Werner E. van Zyl*](#), and [C. W. Liu*](#)

Journal of the American Chemical Society > Vol 146/Issue 1 > Article

[Subscribed](#)

  
Cite Share Jump to

ARTICLE | December 28, 2023

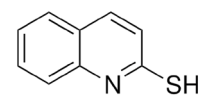
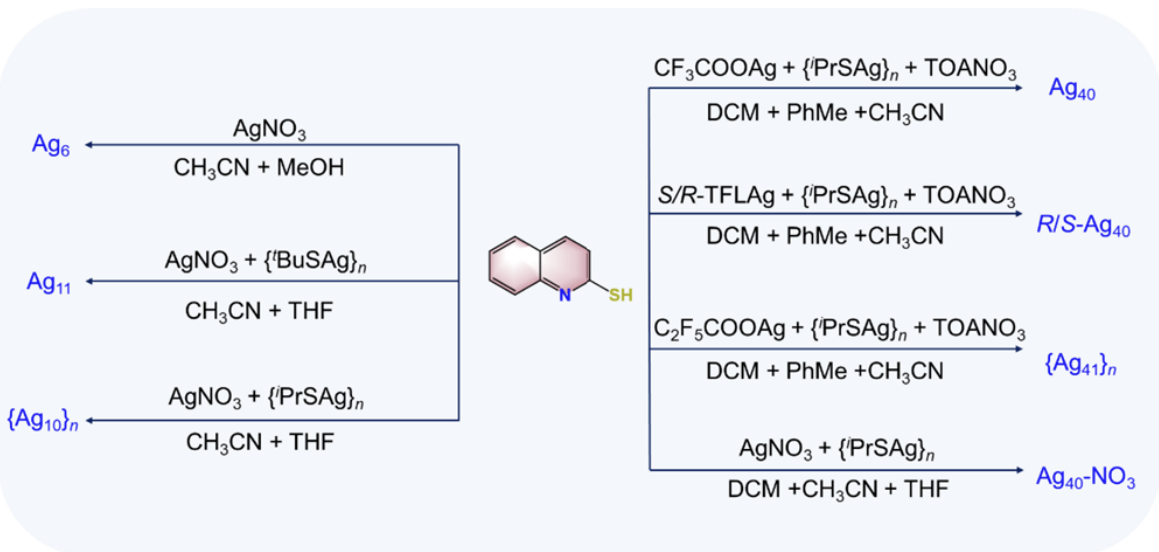
Evolution of Polynuclear Gold(I) Sulfido Complexes from Clusters and Cages to Macrocycles

[Liang-Liang Yan](#), and [Vivian Wing-Wah Yam*](#)

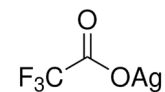
Why this paper?

- Reveals a detailed understanding of the construction of hierarchical crystalline superstructures of large-sized metal NCs from a small building block nanocluster (NC)
- The significance of metal salts, and peripheral ligands of NCs on the transformation of Ag nanowheel to complex triple and double helical superstructures and 1D chains
- Specific biomolecule recognition of Ag₄₀ nanowheel through non-covalent interaction
- Role of solvent in inducing chirality in superstructures

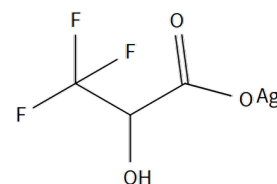
Results & discussion



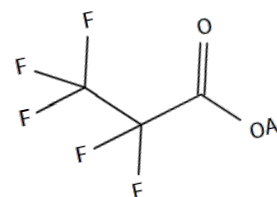
Quinoline-2-thiol [QL-2-SH]



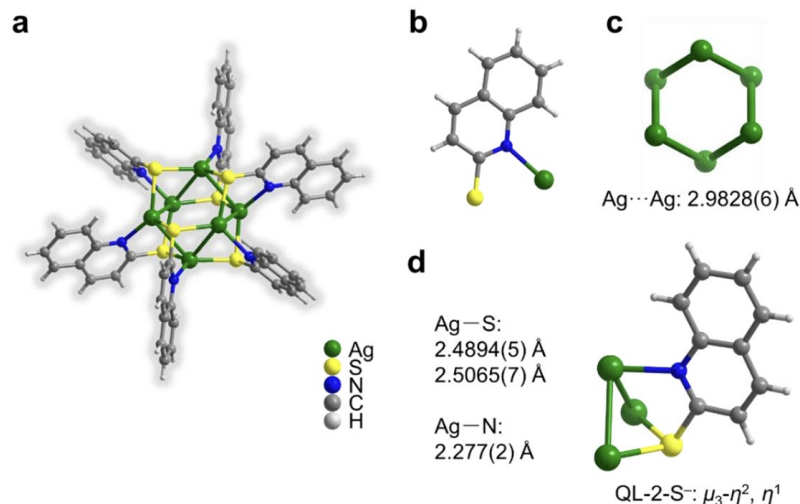
Silver trifluoro acetate



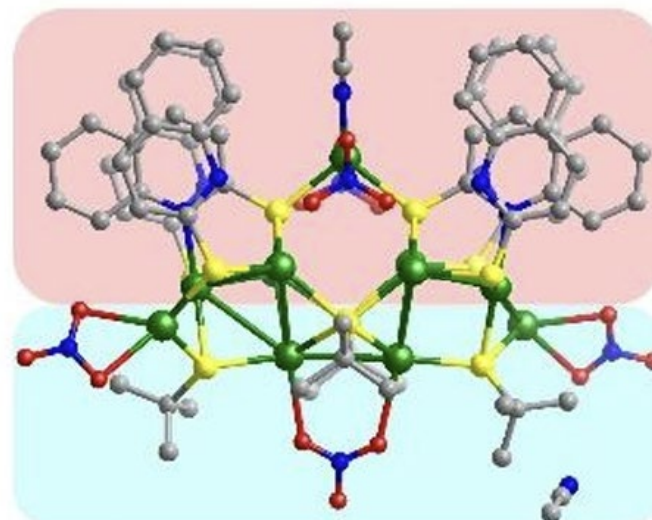
S/R- silver trifluorolactate



C₂F₅COOAg

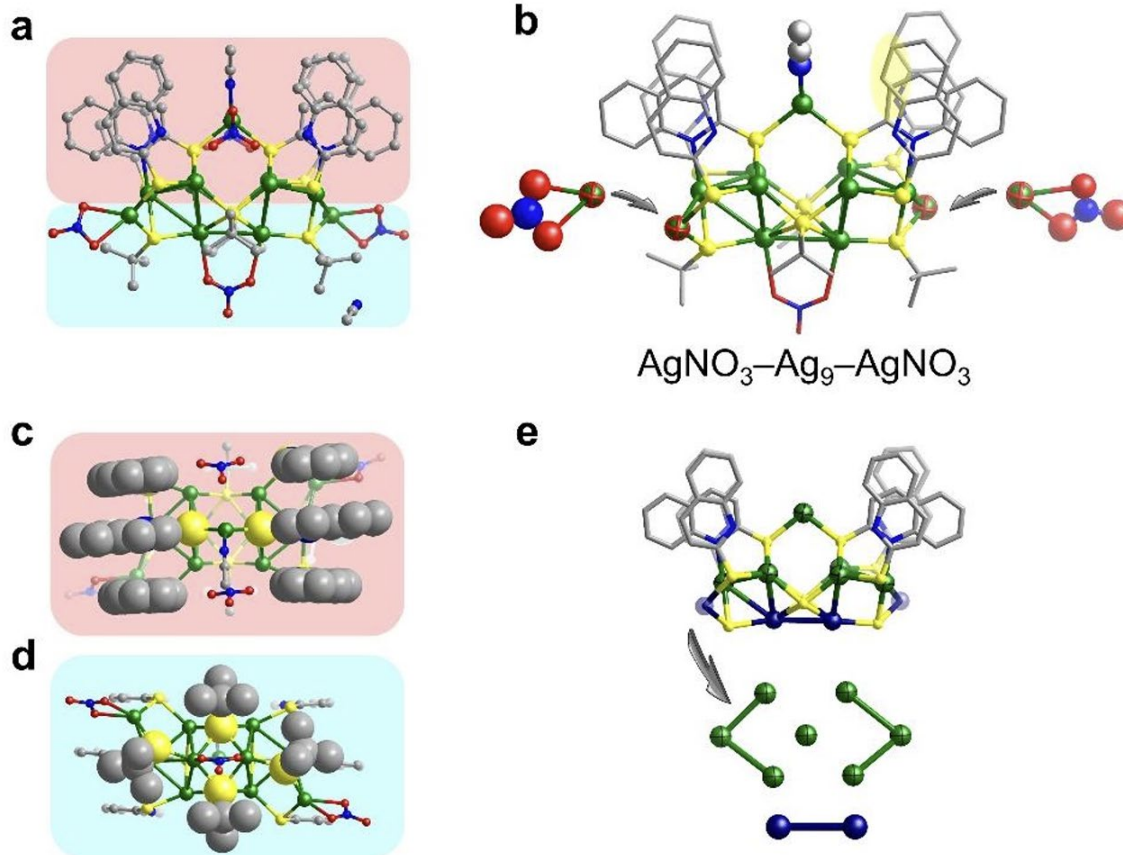


S4. structure analysis for Ag₆(QL-2-S)₆ (Ag₆) based on SCXRD.



S5. Crystal structure of Ag₁₁

Results & discussion



S5. Crystal structure of Ag_{11} . (a) The total structure of Ag_{11} , $\text{Ag}_{11}(\text{QL-2-S})_2(\text{HQL-2-S})_4(\text{tBuS})_4(\text{NO}_3)_5(\text{CH}_3\text{CN})\cdot\text{CH}_3\text{CN}$, where their thiol ligands with different steric hindrance exhibit a 'Janus' distribution mode. (b) Two AgNO_3 as capping agents located on both sides of the Ag_9 building block in Ag_{11} . (c) Six quinoline-2-thiol ligands including 2 QL-2-S- and 4 HQL-2-S, distributed on the same side of Ag_{11} . (d) Four tBuS- ligands distributed on the same side of Ag_{11} . (e) Ag_2 (dark blue) and Ag_7

Results & discussion

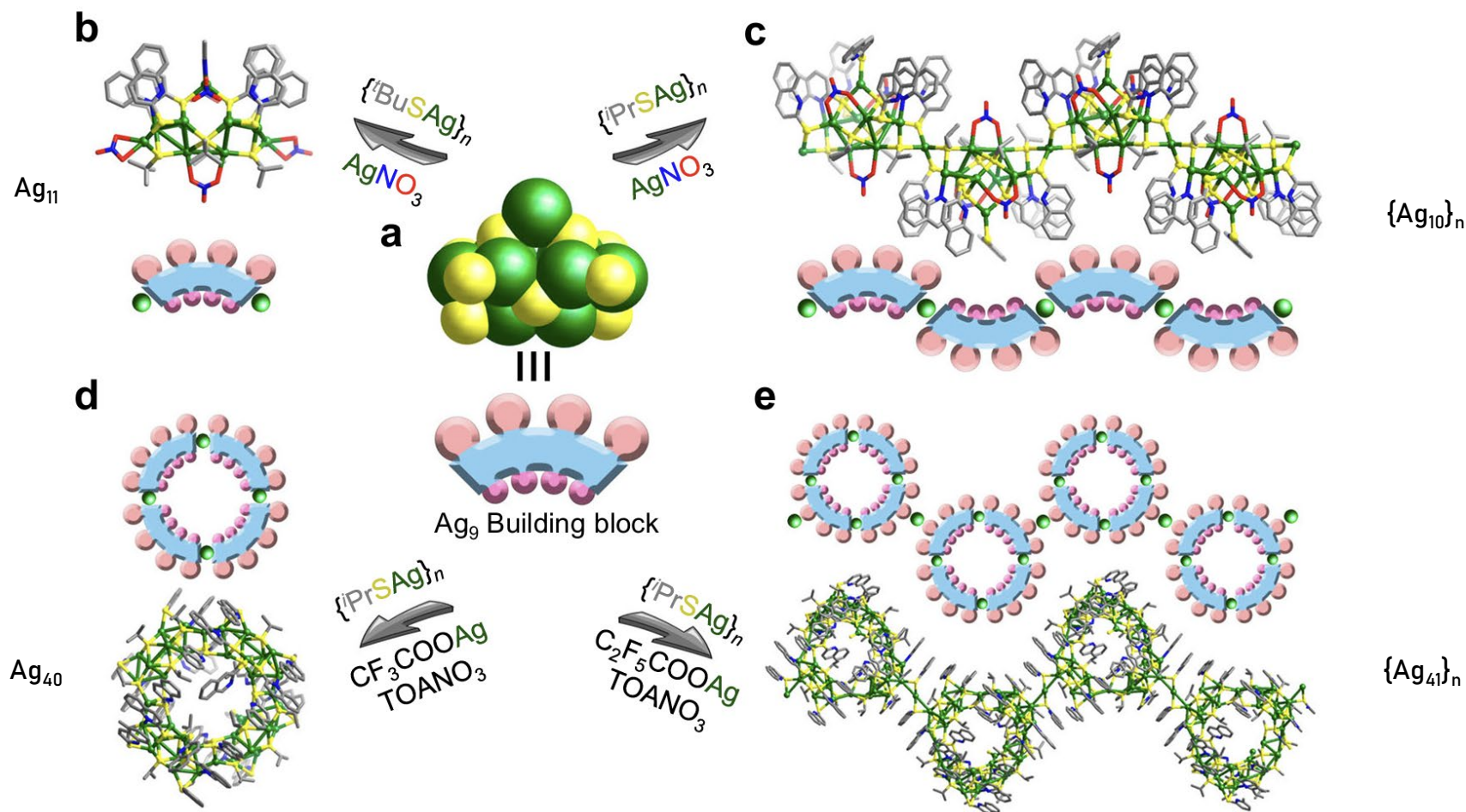
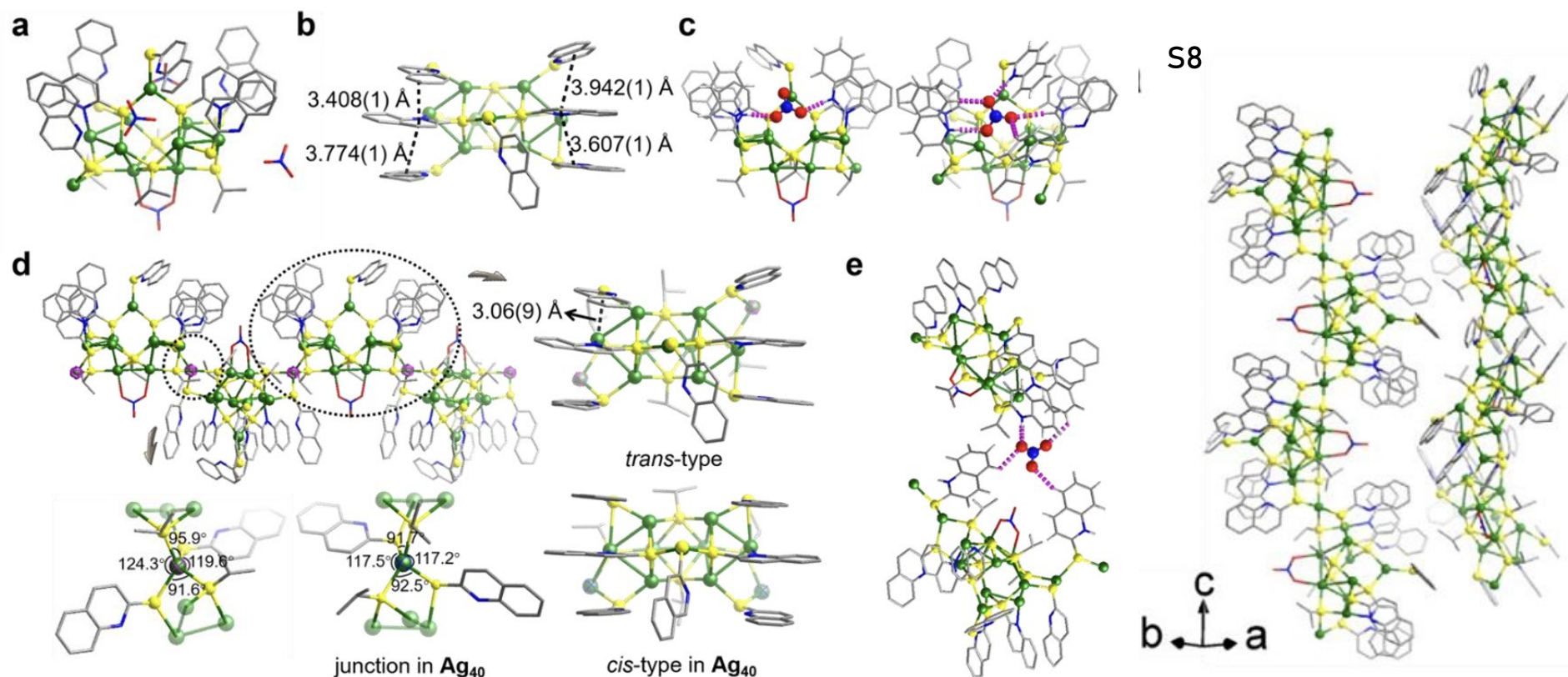


Fig. 1 Hierarchical assembly based on Ag_9 PBBs. a Ag_9 building block, protected by two types of thiol ligands. b Monomer Ag_{11} , blocked by two AgNO_3 molecules at both ends, inhibited further aggregation. c One-dimensional aggregate $\{\text{Ag}_{10}\}_n$, where Ag_9 PBBs are connected by Ag^+ ions to form an infinite structure. d Tetramer Ag_{40} nanowheel, in which four PBBs are gathered together through the silver nodes to form a discrete structure. e One-dimensional aggregate $\{\text{Ag}_{41}\}_n$, in which Ag_{40} nanowheels are connected by additional Ag atoms to form an infinite structure.

Results & discussion



S7. Crystal structure of $\{Ag_{10}\}_n$. (a) Asymmetric unit, $\{Ag_{10}(QL-2-S)_2(HQL-2-S)_5(iPrS)_4(NO_3)_4\}_n$. (b) Intramolecular face-to-face $\pi \cdots \pi$ stacking interactions. (c) NO_3^- anions confined in local cavity between the HQL-2-S ligands via electrostatic interaction, $N(sp^2)-H \cdots O$, $C(sp^2)-H \cdots O$ interactions and weak coordination. (d) The differences between the junctions, Ag_9 building block and connection types in $\{Ag_{10}\}_n$ and Ag_{40} . S8. Packing structures of $\{Ag_{10}\}_n$ in single crystals.

Results & discussion

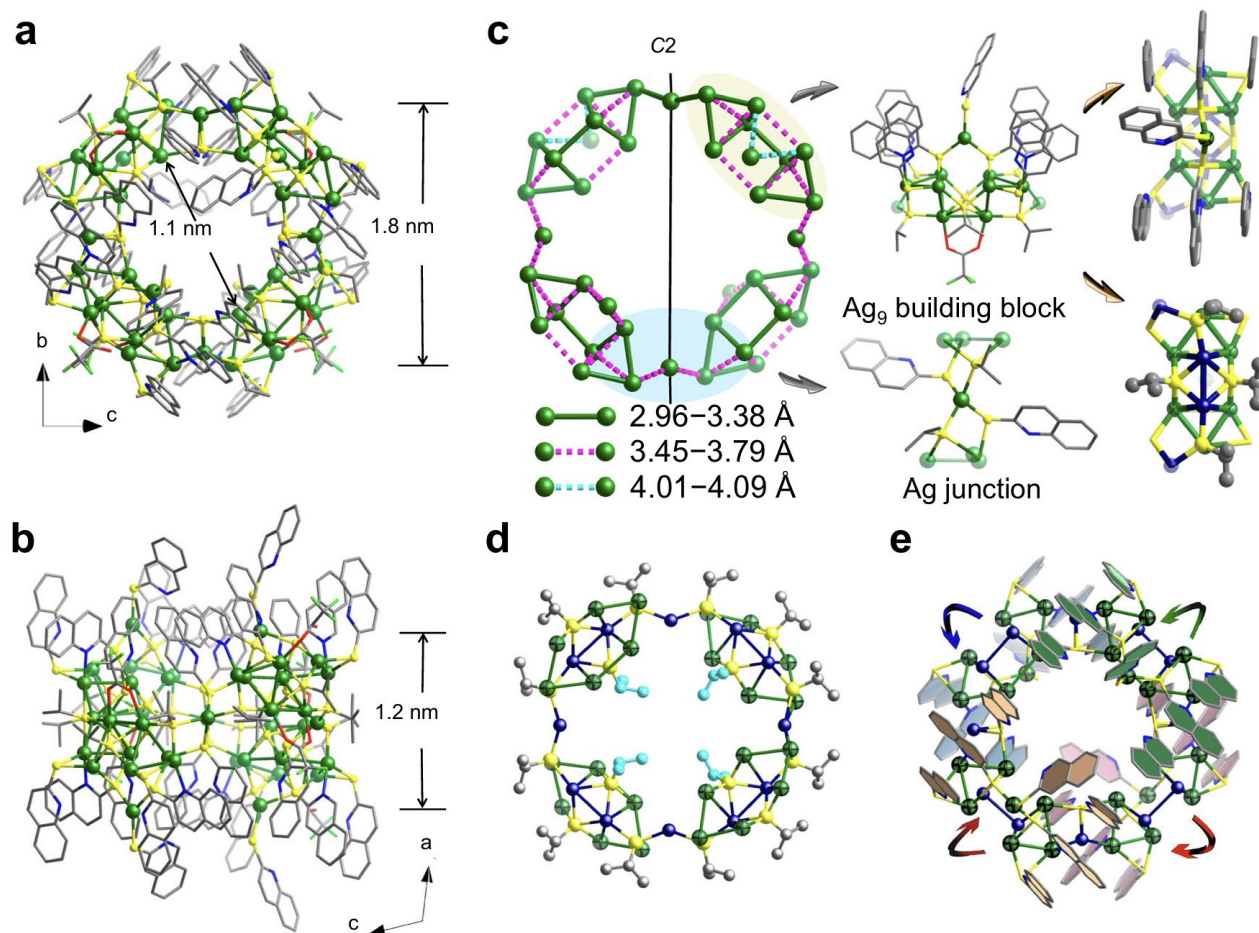
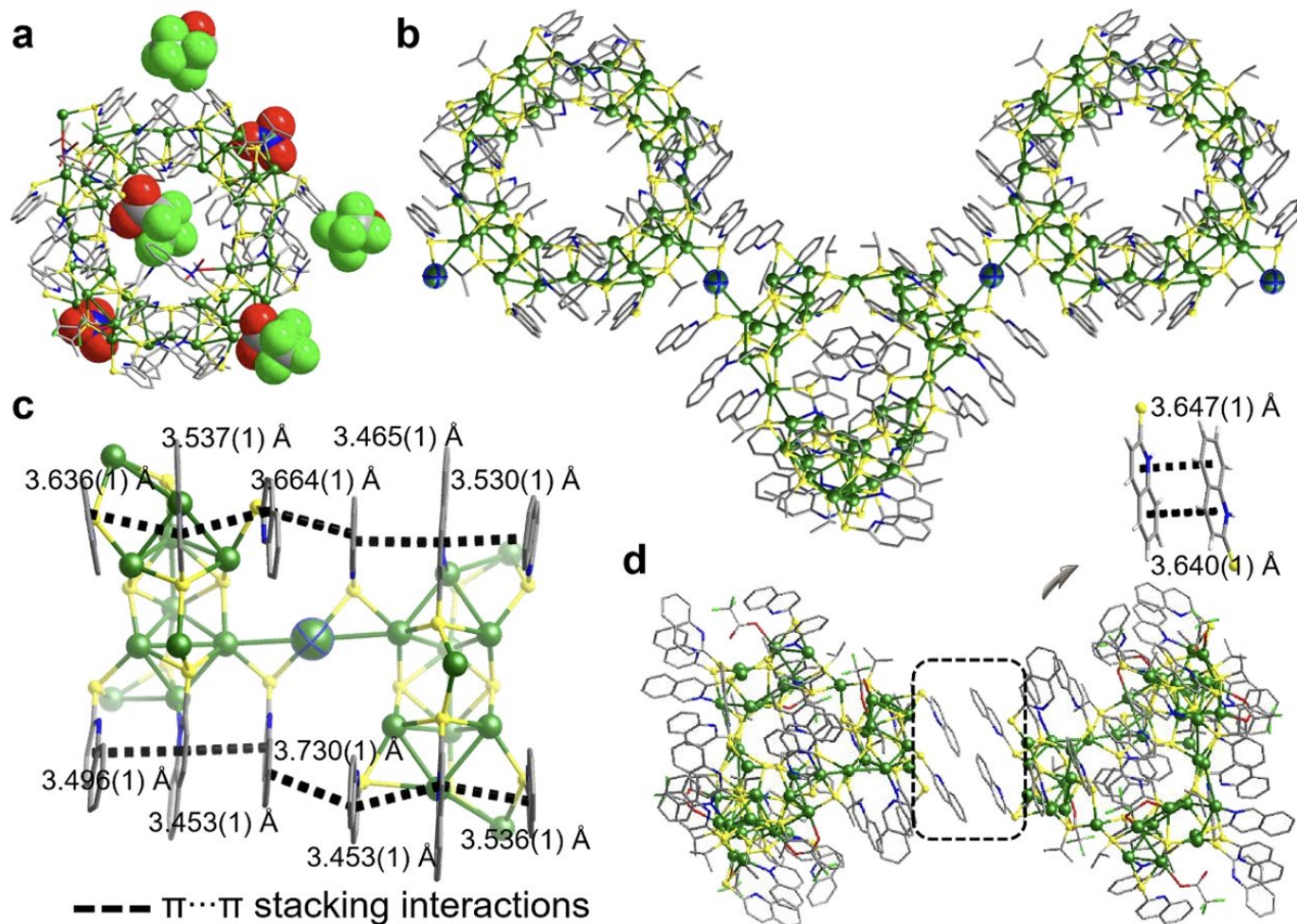


Fig. 2 Crystal structures of Ag_{40} . a,b View of nanowheel Ag_{40} in the a -axis (a) and b -axis (b) directions. c Metal skeleton with a C_2 symmetry of Ag_{40} , constructed by four $[\text{Ag}_9(\text{QL-2-S})_2(\text{HQL-2 S})_5(\text{iPrS})_4(\text{CF}_3\text{COO})]^{2+}$ PBBs (Ag_9 , pale yellow shadow) and four $[\text{Ag}(\text{iPrS})_2(\text{HQL-2 S})_2]^-$ junctions (pale blue shadow). d Distribution of small sterically hindered iPrS^- ligands on the metal skeleton of Ag_{40} , highlighting the four iPrS^- ligands inside the nanowheel (blue) and a ring composed of 12 metal atoms in almost the same plane (dark blue). e Distribution of quinoline-2-thiol ligands with larger steric hindrance on the metal skeleton of Ag_{40} , highlighting the ligands on different PBBs in different colors. .

Results & discussion



S9. Crystal structure of $\{Ag_{41}\}_n$. (a) Asymmetric unit of $\{Ag_{41}\}_n$. (b) One-dimensional aggregate $\{Ag_{41}\}_n$, in which Ag_{40} nanowheels are connected by additional Ag atoms (front ellipses style with blue inner lines) to form an infinite structure. (c) Intrachain face-to-face $\pi\cdots\pi$ stacking interactions. (d) Intermolecular face-to-face $\pi\cdots\pi$ stacking interactions of Ag_{40} .

Results & discussion

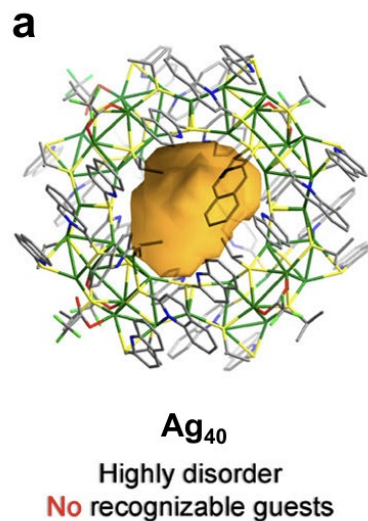
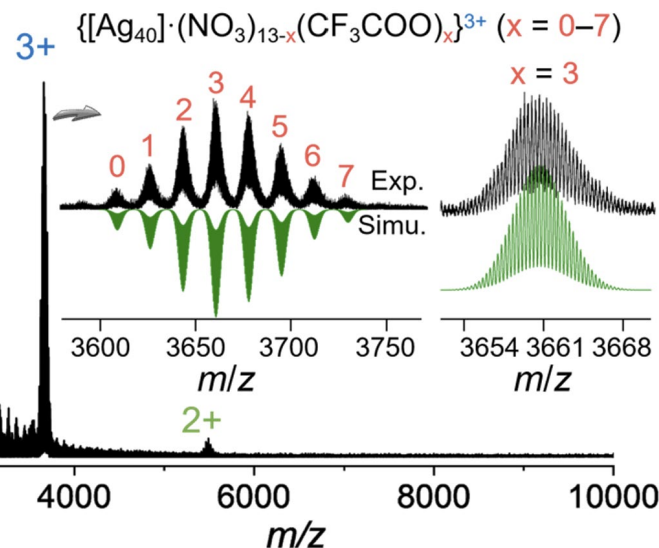
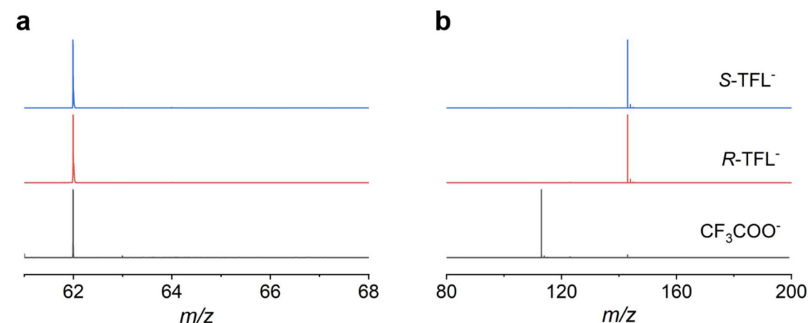


Fig. 3 a Ag₄₀ with an internal nanospace.



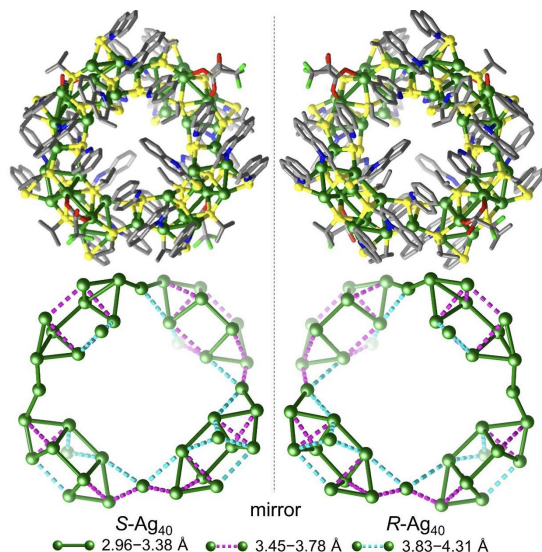
S23. ESI-MS of Ag₄₀ dissolved in DCM collected in positive mode.

	$\{[Ag_{40}(QL-2-S)_8(HQL-2-S)_{20}(iPrS)_{16}(NO_3)_{13-x}(CF_3COO)_x]\}^{3+}$ ($x = 0-7$)
0	$\{Ag_{40}(QL-2-S)_8(HQL-2-S)_{20}(iPrS)_{16}(NO_3)_{13}\}^{3+}$
1	$\{Ag_{40}(QL-2-S)_8(HQL-2-S)_{20}(iPrS)_{16}(NO_3)_{12}(CF_3COO)_1\}^{3+}$
2	$\{Ag_{40}(QL-2-S)_8(HQL-2-S)_{20}(iPrS)_{16}(NO_3)_{11}(CF_3COO)_2\}^{3+}$
3	$\{Ag_{40}(QL-2-S)_8(HQL-2-S)_{20}(iPrS)_{16}(NO_3)_{10}(CF_3COO)_3\}^{3+}$
4	$\{Ag_{40}(QL-2-S)_8(HQL-2-S)_{20}(iPrS)_{16}(NO_3)_9(CF_3COO)_4\}^{3+}$
5	$\{Ag_{40}(QL-2-S)_8(HQL-2-S)_{20}(iPrS)_{16}(NO_3)_8(CF_3COO)_5\}^{3+}$
6	$\{Ag_{40}(QL-2-S)_8(HQL-2-S)_{20}(iPrS)_{16}(NO_3)_7(CF_3COO)_6\}^{3+}$
7	$\{Ag_{40}(QL-2-S)_8(HQL-2-S)_{20}(iPrS)_{16}(NO_3)_6(CF_3COO)_7\}^{3+}$

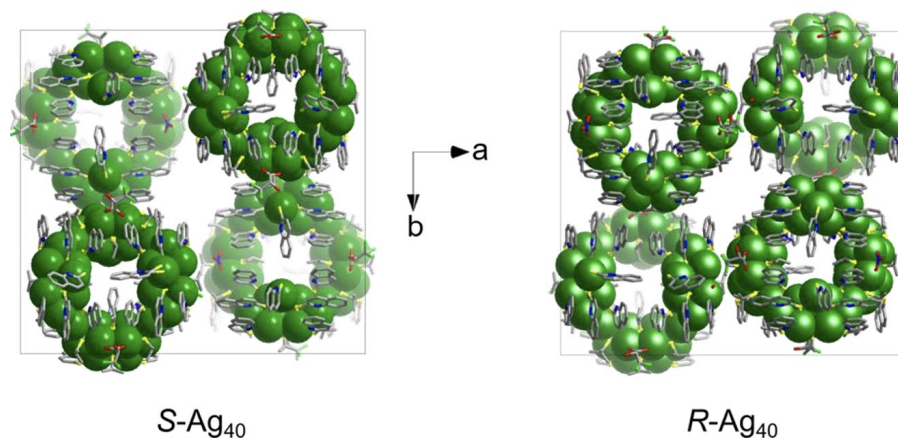


S23. Mass spectrum of Ag₄₀ and S-/R-Ag₄₀ in negative-ion mode, confirming the presence of NO₃⁻ (a), CF₃COO⁻ and S-/R-TFL⁻ (b)

Results & discussion



S19. Ball-and-stick representation of the enantiomers and their metal skeletons of S-Ag₄₀ and R-Ag₄₀.



S20. Unit cells of S-Ag₄₀ (a) and R-Ag₄₀ (b), in which exist four chiral nanowheel molecules.

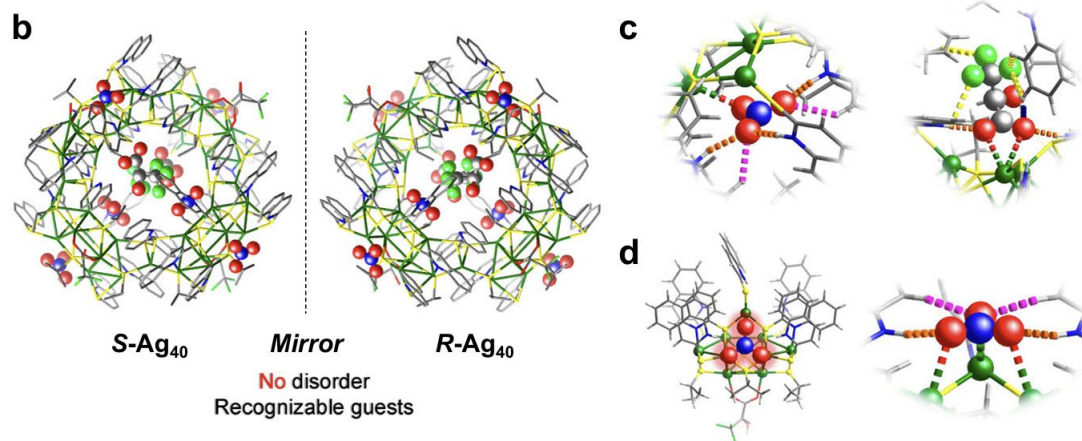


Fig. 3 b S-Ag₄₀ and R-Ag₄₀ nanowheels with C_1 symmetry, S-Ag₄₀ and R-Ag₄₀ display the chiral structure and the non-coordinated guest anions (NO_3^- and S-/R-TFL⁻) in the internal nanospace. c, d Non-coordinated guest anions confined in the internal or outer nanospace via hydrogen bonding and weak coordination.

Results & discussion

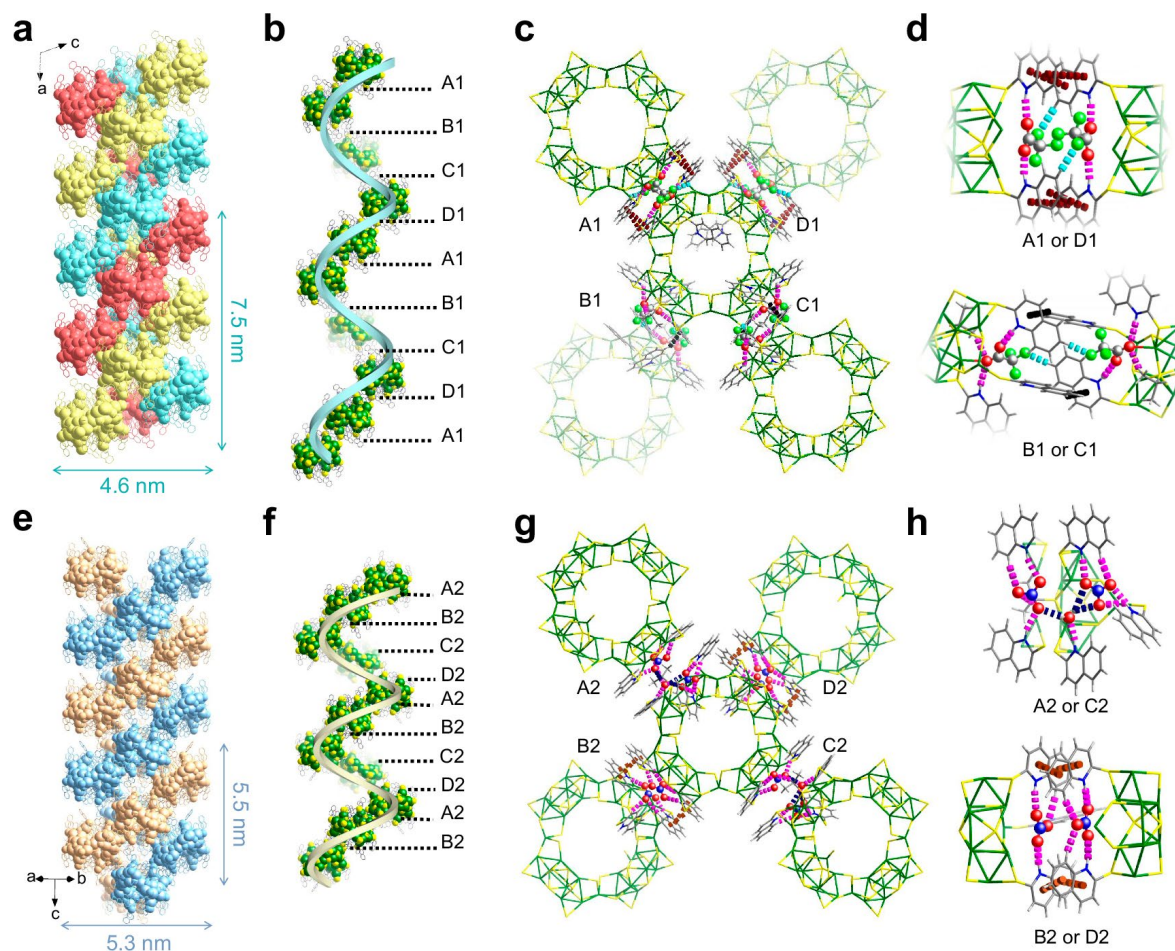
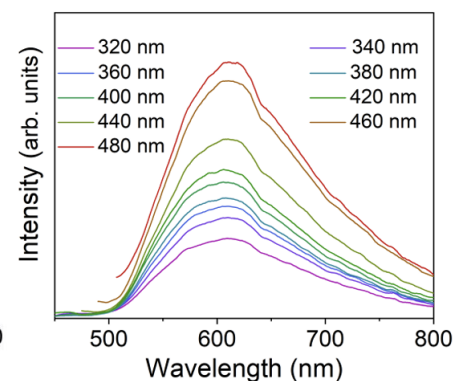
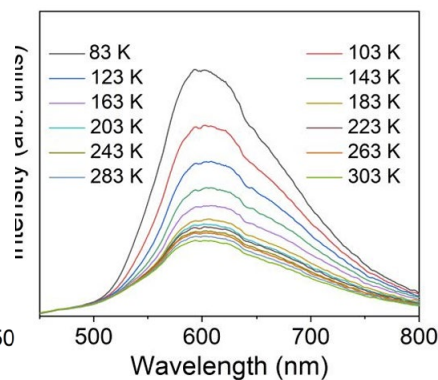
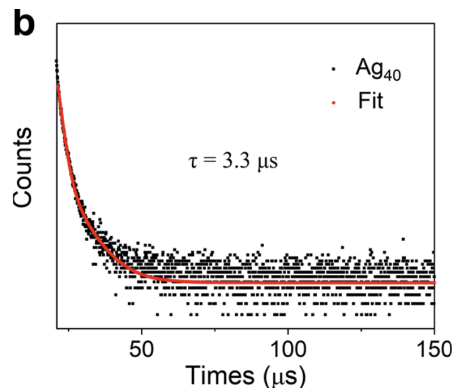
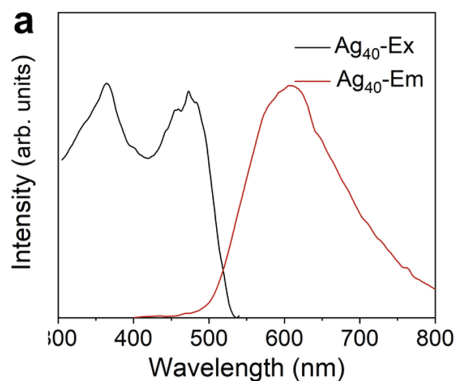
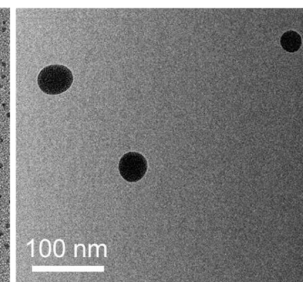
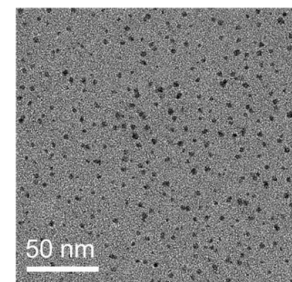
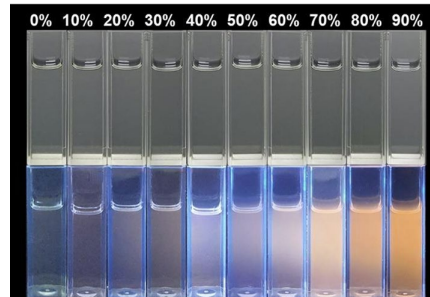
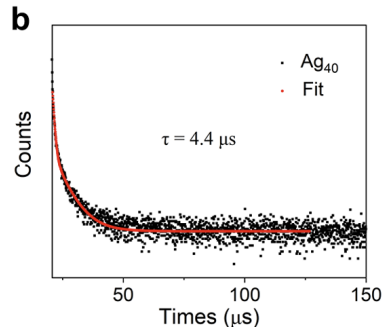
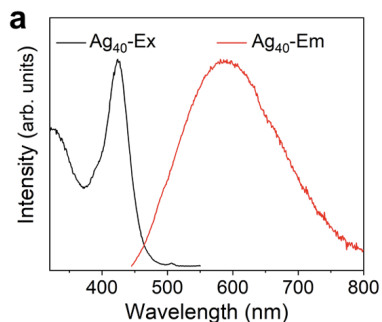
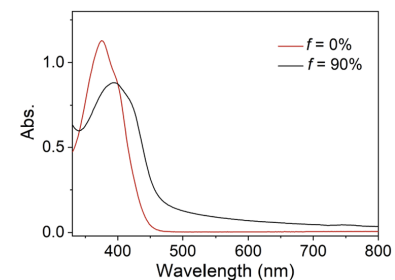
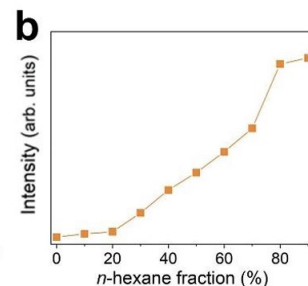
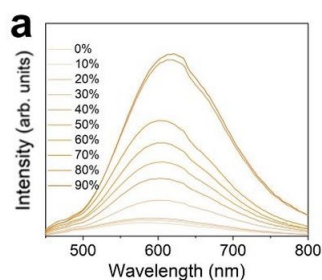
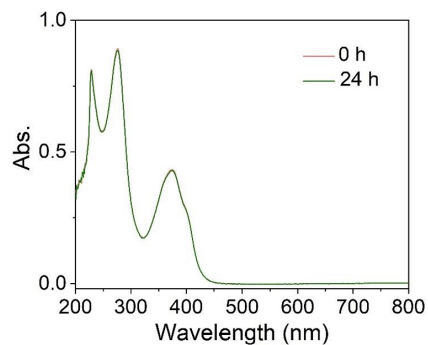


Fig. 4 a Self-assembly of Ag_{40} NCs into a triple-helical structure. b Helical linear chain of the triple-helical superstructure oriented and connected by two different surface motif pairs of Ag_{40} (A1/D1 and B1/C1). c Four types of motif matching between the neighboring nanowheels in the Ag_{40} supercrystal. d Intermolecular interactions of the two different surface motif pairs of Ag_{40} . e Self-assembly of S-Ag_{40} NCs into a double-helical structure. f Helical linear chain of the double-helical superstructure is orientally connected by two different surface motif pairs of S-Ag_{40} (A2/C2 and B2/D2). g Four types of motif matching between neighboring nanowheels in the S-Ag_{40} supercrystal. h Intermolecular interactions of two different surface motif pairs of S-Ag_{40}

Results & discussion

Aggregation-induced emission enhancement (AIEE) behavior



Results & discussion

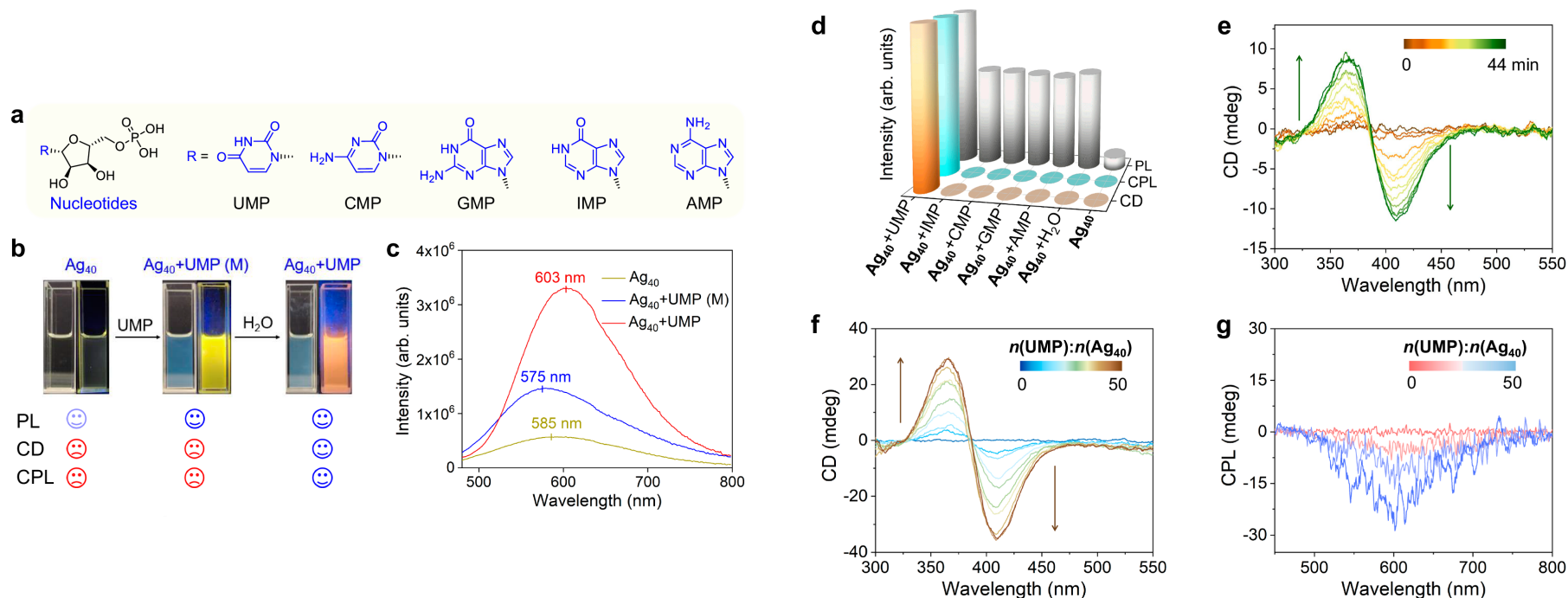


Fig. 5 a Molecular structure of various nucleotides. b CD and CPL activities triggered by the co-assembly process of Ag_{40} in DCM with UMP (dissolved in DMSO) and H_2O c Emission spectra of different stages (initial, Ag_{40} ; intermediate, $\text{Ag}_{40} + \text{UMP}$ (M); final, $\text{Ag}_{40} + \text{UMP} + \text{H}_2\text{O}$, abbreviated as $\text{Ag}_{40} + \text{UMP}$) in the recognition ($\lambda_{\text{ex}} = 430 \text{ nm}$). d Column chart of the emission intensity of the PL, CD, and CPL spectra for Ag_{40} , $\text{Ag}_{40} + \text{H}_2\text{O}$, and the co-assemblies with nucleotides. e Time-dependent CD spectra of the co-assemblies formed by Ag_{40} ($1 \times 10^{-5} \text{ mol L}^{-1}$) in 3 mL of DCM with 20 μL of UMP ($3 \times 10^{-2} \text{ mol L}^{-1}$) in DMSO and 20 μL of H_2O . Interval: 4 min. f CD spectra of the co-assemblies formed by Ag_{40} ($1 \times 10^{-5} \text{ mol L}^{-1}$) in 3 mL of DCM with 0–50 μL of UMP ($3 \times 10^{-2} \text{ mol L}^{-1}$) in DMSO and 20 μL of H_2O . Interval: 5 μL . g CPL spectra of the co-assemblies formed by Ag_{40} ($1 \times 10^{-5} \text{ mol L}^{-1}$) in 3 mL of DCM with 0–50 μL of UMP ($3 \times 10^{-2} \text{ mol L}^{-1}$) in DMSO and 20 μL of H_2O . Interval: 5 μL .

Results & discussion

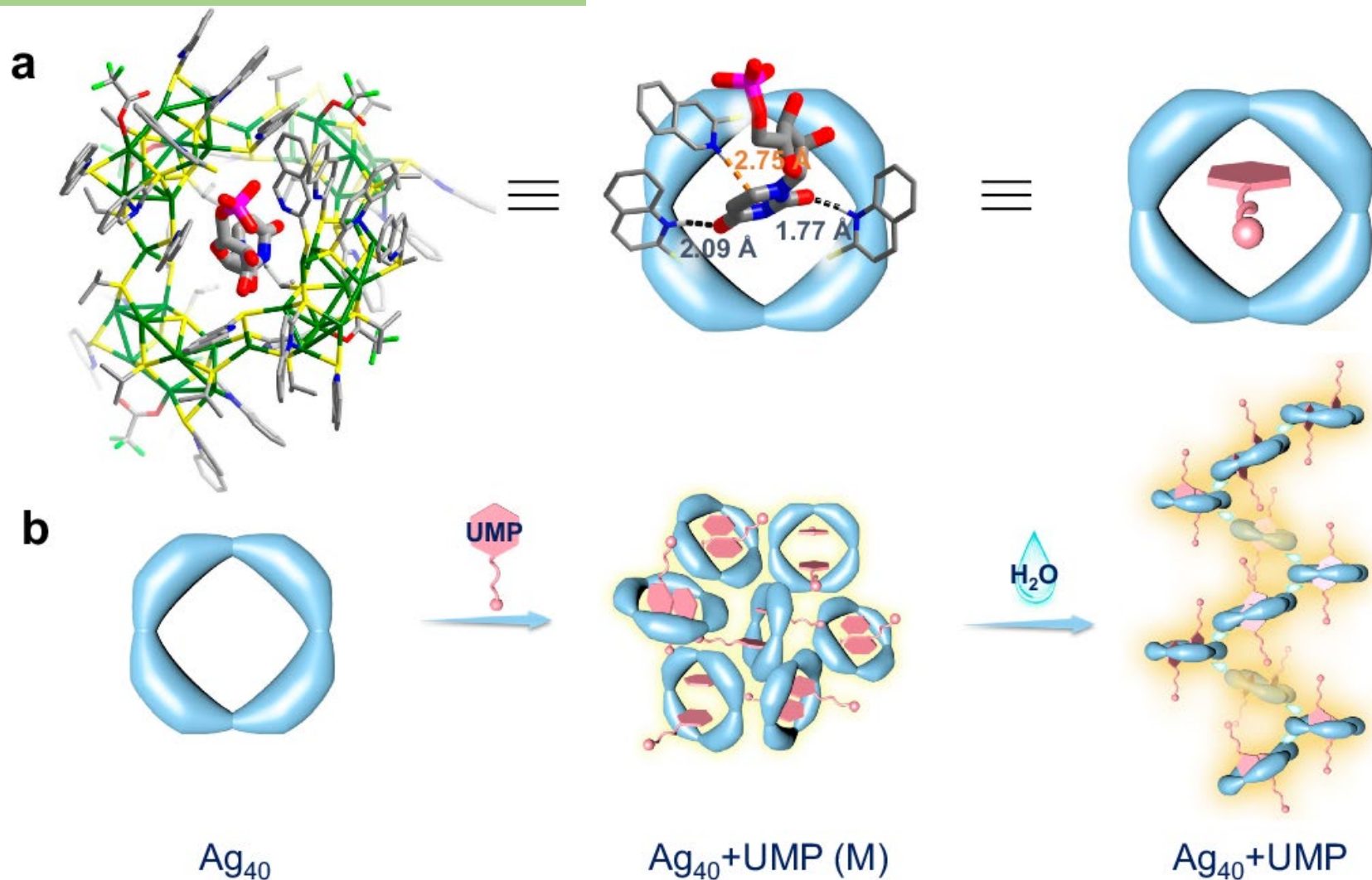


Fig. 6 a DFT (PBE0/def2-SVP)-calculated structure of the Ag_{40} and UMP co-assembly, dotted lines indicate non-covalent interactions, including N-H \cdots O (black line) and N-H \cdots π (orange line). Color codes: Ag green, S yellow, C gray, N blue, F cyan, O red, H white. b Scheme showing the chiral co-assembly process of Ag_{40} and UMP mediated by H_2O .

Conclusion

- It developed a series of molecules from small NCs like Ag_6 , Ag_{11} to one-dimensional $\{\text{Ag}_{10}\}_n$ chain, tetrameric Ag_{40} nanowheel, S/R- chiral Ag_{40} nanowheel, 1D chain of $\{\text{Ag}_{41}\}_n$ based on primary building blocks Ag_9
- Formation of triple and double-helical assembly of Ag_{40} nanowheel by regulating the surface anions of the NCs
- It shows how subtle changes in solvent, and surface anions can regulate the formation of complex hierarchical structure
- Specific co-assembly formation of Ag_{40} nanowheel with UMP nucleotide and induction of chirality into the co-assembly mediated by water